

Observation of the Conductivity Coherence Peak in Superconducting $\text{Bi}_2\text{Sr}_2\text{CaCu}_2\text{O}_8$ Single Crystals

K. Holczer,^{(1),(a)} L. Forro,⁽²⁾ L. Mihály,⁽²⁾ and G. Grüner⁽¹⁾

⁽¹⁾ *Physics Department and Solid State Science Center, University of California, Los Angeles, Los Angeles, California 90024*

⁽²⁾ *Department of Physics, State University of New York at Stony Brook, Stony Brook, New York 11794-3800*

(Received 17 January 1991)

We have measured the surface impedance of $\text{Bi}_2\text{Sr}_2\text{CaCu}_2\text{O}_8$ single crystals and have evaluated the conductivity σ_1 at millimeter-wave frequencies. We observe a peak below T_c which we suggest is due to case-II coherence factors, like the Hebel-Slichter peak observed in the NMR relaxation rate of classical superconductors. A comparison with theory leads to a large gap, suggesting strong coupling.

PACS numbers: 74.30.Gn

In spite of a significant amount of experimental and theoretical work, the nature of the superconducting state in various high- T_c materials remains controversial. Penetration-depth experiments strongly favor s -wave pairing,¹ and the temperature dependence of the NMR Knight shift² is also in agreement with this interpretation. However, no coherence peak (the so-called Hebel-Slichter peak) has been found³ in the NMR relaxation rate $1/T_1$, in clear contrast to what is predicted for conventional, BCS-type behavior. The value of the superconducting gap Δ and the question of whether states exist below the gap for $T < T_c$ are also not resolved, although it is generally agreed⁴ that the strong-coupling limit applies and 2Δ well exceeds the weak-coupling value $2\Delta/k_B T_c = 3.52$.

The electrodynamic of the superconducting state is, similarly to the NMR relaxation rate, characterized by case-II coherence factors,⁵ and consequently in the case of s -wave pairing, a peak is expected in the temperature dependence of σ_1 , the real part of the complex conductivity $\sigma = \sigma_1 + i\sigma_2$, at temperatures somewhat below T_c . Although the conductivity coherence peak had not been evaluated⁶ (due to technical difficulties discussed below) during the period when the electrodynamic of conventional superconductors were explored,⁷ we have shown recently⁸ that for superconducting Pb the coherence peak can be readily evaluated.

In this Letter we report on our experiments on $\text{Bi}_2\text{Sr}_2\text{CaCu}_2\text{O}_8$ crystals. We find a well-defined coherence peak, clearly demonstrating that pairing is dominantly s wave. Furthermore, our experiments suggest a large superconducting gap.

Single crystals of nominal composition $\text{Bi}_2\text{Sr}_2\text{CaCu}_2\text{O}_8$ have been grown from a mixture of BiO , $\text{Sr}_2\text{O}_3\text{CaCO}_3$, and CuO . The Bi:Sr:Ca:Cu ratio of the starting materials was 2:2:1:3, and components of analytic purity were used. The mixture was poured into an alumina crucible, brought to 800°C , and kept at this temperature for 10 h. Then the temperature was increased to 1020°C , and the liquid was mixed thoroughly. The total volume of the melt was approximately 10 cm^3 . The crystals were grown during a cooling from this temperature with a

cooling rate of $2^\circ\text{C}/\text{h}$. The cooling rate was increased to $10^\circ\text{C}/\text{h}$ after the temperature reached 790°C . The product of this process is an ingot containing large single crystals of $\text{Bi}_2\text{Sr}_2\text{CaCu}_2\text{O}_8$ (2:2:1:2), embedded in a matrix consisting of a CuO -rich phase. The composition of the crystals has been investigated by x-ray fluorescence and the structure was studied by electron and x-ray diffraction.^{9,10} The samples have a pseudotetragonal structure with $a = b = 5.36\text{ \AA}$ and a superlattice of period $4.7b$ in the b direction. Hall effect,¹⁰ infrared transmission,¹¹ thermopower, S - I - S tunneling, and other studies were performed on the samples produced by this method. For the experiments reported here, the crystals were selected from different batches, cleaved to the appropriate size, and subjected to a heat treatment in air at 600°C for 10–20 min. This treatment is required for obtaining reproducible superconducting transition temperatures; the thinner the samples, the shorter the annealing time that is sufficient. After heat treatment each sample was cut into two pieces; one of them was used in the microwave study, and dc resistivity was measured on the other. For samples from the same batch, T_c was within a 3-K range; samples from different batches have a range of critical temperatures of $T_c(\text{dc}) = 80\text{--}92\text{ K}$. The critical temperatures reported in this paper correspond to the zero-dc-resistivity state of the samples.

Our experiments were conducted at $f = 60\text{ GHz}$ using a resonant cavity operating in the TE_{011} mode, with the specimen placed inside the cavity in a maximum ac magnetic field H_{ac} (with the electric field E_{ac} ideally zero) or in a maximum electric field E_{ac} (for which H_{ac} is zero). For both configurations the single-crystal platelets were oriented to result in the shielding-current flow (for ideal orientation) parallel to the conducting layers, and consequently the in-plane electrodynamic is examined. For the maximum- H_{ac} configuration, the applied field is perpendicular to the layers, while for the maximum- E_{ac} configuration, it is parallel to the layers; both configurations are displayed in Fig. 2. The experimental technique was described earlier.⁸

For specimens for which the skin depth δ and/or the penetration depth λ is smaller than the dimensions, the

parameter which determines the modification of the resonance characteristics when the specimen is inserted is called the surface impedance.¹²

$$Z_s = R_s + iX_s = \left(\frac{\mu_0 \omega}{\sigma_1 - i\sigma_2} \right)^{1/2}, \quad (1)$$

with R_s and X_s the surface resistance and surface reactance, respectively. R_s is proportional to the excess loss and, consequently, to the inverse quality factor Q^{-1} , or alternatively, the half-width of the resonance, while X_s is proportional to the frequency shift Δf_0 which occurs when the sample is placed inside the cavity:

$$\Delta f_0 = \frac{1}{2} A (X_s + X_s^0), \quad \Delta(1/Q) = A R_s, \quad (2)$$

where A depends on the dimensions of the cavity and the specimen under investigation. The parameter A is not required in the analysis of the superconducting-state properties, as the relevant quantities which can be compared with theory are X_s and R_s in the superconducting state relative to these parameters in the normal state, i.e., X_N and R_N , and A does not enter into these ratios. The parameter X_s^0 reflects small differences in the cavity dimension resulting from unavoidable differences in the way the resonant structure is assembled for the different experimental runs. One can, however, evaluate X_s^0 by employing certain relations between R_s and X_s in certain limits. In Fig. 1 we display the temperature dependence of R_s and X_s with both parameters normalized to their $T=100$ K value. The temperature-independent numerical constant X_s^0 has been evaluated in the following way. In the normal state above T_c , and in the so-called Hagen-Rubens limit ($\omega\tau < 1$ with τ the single-particle

relaxation time), Eq. (1) leads to

$$R_s = X_s = (\mu_0 \omega / 2\sigma_1)^{1/2}. \quad (3)$$

In other words, both R_s and X_s are expected to have the same value at all temperatures in the normal state. Optical experiments give a relaxation time $1/\tau \sim 500 \text{ cm}^{-1}$ at $T=100$ K and larger $1/\tau$ values at higher temperatures, and consequently, the Hagen-Rubens limit applies at our measurement frequency.¹¹ We can then use Eq. (3) to establish the additive frequency shift Δf_0^0 , or alternatively, X_s^0 by requiring that $X_s = R_s$ in the normal state, and data presented in Fig. 1 have been obtained in this way. The observation that the temperature dependence of X_s follows that of R_s in the entire measured temperature range $T > T_c$ clearly demonstrates that the Hagen-Rubens limit applies, and strongly supports our procedure for evaluating X_s^0 .

Turning to the superconducting state, we observe a dramatic drop of R_s below the transition, and $R_s \rightarrow 0$ as $T \rightarrow 0$ within our resolution. X_s , while decreasing below T_c , remains constant at temperatures well below T_c .

With the R_s and X_s values shown in Fig. 1 we can use Eq. (1) to evaluate σ_1 and σ_2 . As discussed earlier, from Eq. (2) it follows that we can evaluate these components only up to a numerical factor A . This factor, however, depends only on the dimensions of the specimens and is the same for conductivity values both below and above T_c . Consequently, this factor is eliminated if R_s/R_N , X_s/X_N , or σ_1/σ_N is derived. In Fig. 2 we display σ_1/σ_N as a function of temperature using two different geometrical configurations, where the specimen was placed in a maximum electric or in a maximum magnetic field. The close similarity of the two results strongly suggests that demagnetization effects and finite-magnetic-field-

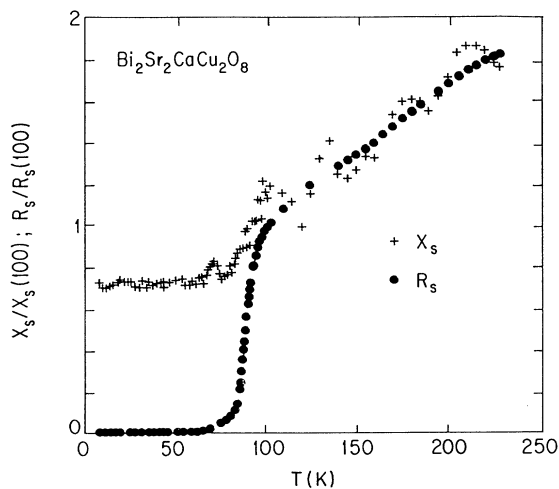


FIG. 1. Temperature dependence of the surface resistance and surface reactance for $\text{Bi}_2\text{Sr}_2\text{CaCu}_2\text{O}_8$ for a maximum- H_{ac} configuration (see text). $T_c^{\text{dc}} = 91$ K, as evaluated from dc resistivity.

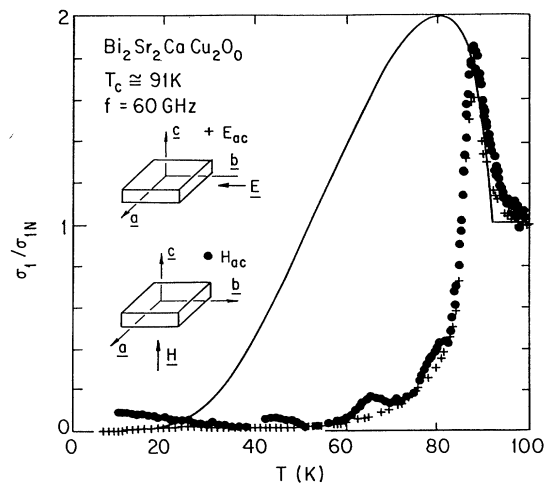


FIG. 2. Temperature dependence of σ_1 as evaluated using a maximum- E_{ac} and a maximum- H_{ac} configuration. The measurement configurations are also displayed.

induced loss mechanisms (due to losses and increased penetration into the superconductor due to frozen-in flux, for example) do not play a role, and the results displayed on the figure reflect the electrodynamics of the London state.

For both cases σ_N refers to the extrapolated normal-state conductivity evaluated from the temperature dependence of σ_N above 100 K. It is expected that in the case where the material would remain metallic at temperatures below T_c , the conductivity would increase, being approximately inversely proportional to the temperature T . The quantity which should be compared with theory, i.e., $\sigma_1(T)/\sigma_N(T)$, is evaluated this way. The overall qualitative features of the figure are not modified by this effect.

Also shown in Fig. 2 is the conductivity evaluated assuming weak-coupling BCS with finite-mean-free-path corrections.¹³ It is clear that while a coherence peak is recovered by the model, a small single-particle gap is not compatible with our experimental findings. While detailed calculations based on the strong-coupling limit have not been performed, with increasing Δ two modifications occur:¹⁴ The position of the coherence peak moves towards T_c and σ_1 drops more dramatically below the coherence peak. Both are features we observe experimentally, but whether strong-coupling effects fully account for our experimental findings remains to be seen. We also note that higher-angular-momentum pairing leads to a dramatic reduction of the coherence peak¹⁵ and we believe that our experiments rule out ground states with symmetry dramatically different from s wave.

In Fig. 3, experimental results on another specimen with a lower transition temperature, $T_c = 80$ K, and of a lesser quality is displayed. The coherence peak is somewhat broadened, most probably reflecting a distribution of transition temperatures in the specimen. Although we do not have direct evidence for such a distribution of

transition temperatures (the dc resistivity being fairly insensitive to such distribution effects), as a general rule, lower average transition temperatures are related to broader transitions, and to a larger distribution of local T_c values in these materials, making this the most likely explanation of Fig. 3.

In conclusion, we have observed a well-defined peak in the real part of the finite-frequency conductivity σ_1 in the superconducting state of $\text{Bi}_2\text{Sr}_2\text{Ca}_2\text{Cu}_2\text{O}_8$. We believe the observation gives conclusive evidence for a singlet superconducting ground state. A comparison with theory which takes finite-mean-free-path effects into account strongly suggests that the single-particle gap exceeds $\Delta = 1.76kT_c$, the weak-coupling limit. We also note that X_s is, within experimental error, independent of temperature for $T < T_c$ (see Fig. 1) excluding important contributions coming from zeros in the gap function.

The reason why case-II coherence factors are observed in the electrodynamic response but not in the NMR relaxation rate in these materials remains an unresolved issue. There are two important differences between the processes which determine σ_1 and T_1 . First, the conductivity reflects charge-fluctuation effects while the NMR relaxation time is due to spin fluctuations. Second, σ_1 is due to correlations with $q = 0$ while T_1 samples the entire q space; this difference is believed to be important for the normal-state properties. Which of these effects is responsible for the difference between the conductivity and relaxation time remains to be seen.

We wish to thank J. J. Chang and D. J. Scalapino for calculating σ_1 and S. Chakravarty for useful discussions. This research was supported by NSF Grants No. DMR-89-13236 (K.H. and G.G.) and No. DMR-90-16456.

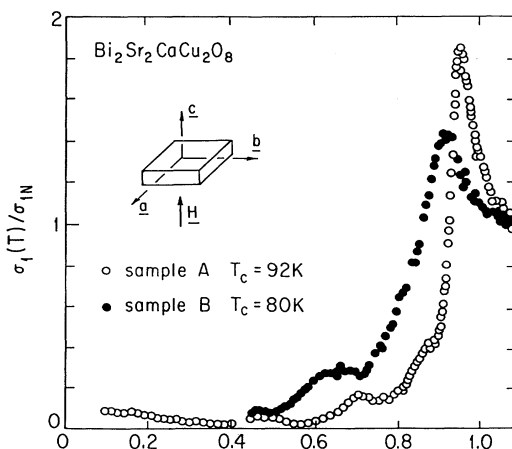


FIG. 3. Temperature dependence of σ_1 evaluated on a second specimen, with a lower transition temperature, $T_c^{\text{dc}} = 80$.

(a)Permanent address: Central Research Institute for Physics, Budapest, Hungary.

¹D. R. Harshman *et al.*, Phys. Rev. B **39**, 851 (1989).

²M. Takigawa *et al.*, Phys. Rev. B **39**, 7371 (1989); S. E. Barrett *et al.*, Phys. Rev. B **41**, 6283 (1990).

³W. W. Warren *et al.*, Phys. Rev. Lett. **58**, 1860 (1987); Y. Kitaoka *et al.*, J. Phys. Soc. Jpn. **57**, 30 (1988); T. Imai *et al.*, J. Phys. Soc. Jpn. **57**, 2280 (1988); P. C. Hammel *et al.*, Phys. Rev. Lett. **63**, 1992 (1989); H. Zimmermann *et al.*, Physica (Amsterdam) **159C**, 681 (1989); K. Fujiwara *et al.*, J. Phys. Soc. Jpn. **58**, 380 (1989).

⁴See, for example, articles in *High Temperature Superconductivity*, edited by K. S. Bedell *et al.* (Addison-Wesley, Redwood City, CA, 1990).

⁵J. R. Schrieffer, *Theory of Superconductivity* (Benjamin/Cummings, New York, 1964).

⁶See, for example, M. S. Khaikin, Zh. Eksp. Teor. Fiz. **34**, 1389 (1958) [Sov. Phys. JETP **7**, 961 (1958)].

⁷H. Tinkham, *Introduction to Superconductivity* (McGraw-Hill, New York, 1975).

⁸K. Holczer, O. Klein, and G. Grüner, Solid State Commun. (to be published).

⁹L. Forro, D. Mandrus, B. Keszei, and L. Mihály, *J. Appl. Phys.* **68**, 4876 (1990).

¹⁰L. Forro, D. Mandrus, C. Kendziora, L. Mihály, and R. Reeder, *Phys. Rev. B* **42**, 8704 (1990).

¹¹L. Forro, G. L. Carr, J. P. Williams, D. Mandrus, and L. Mihály, *Phys. Rev. Lett.* **65**, 1941 (1990).

¹²C. Kittel, *Quantum Theory of Solids* (Wiley, New York, 1963); J. R. Waldram, *Adv. Phys.* **13**, 1 (1964).

¹³J. J. Chang and D. Scalapino, *Phys. Rev.* **40**, 4299 (1989). The full line shown in Fig. 2 has been evaluated for $l/\pi\xi_0=1$, with l the mean free path and ξ_0 the coherence length, and the above ratio is close to the accepted values of l and ξ_0 for various high- T_c superconductors.

¹⁴J. J. Chang (private communication).

¹⁵D. M. Ginsberg and L. C. Hebel, in *Superconductivity*, edited by R. D. Parks (Marcel Dekker, New York, 1969).